

Evaluation of Atomic, Physical, and Thermal Properties of Bismuth Oxide Powder: An Impact of Biofield Energy Treatment

Mahendra Kumar Trivedi¹, Rama Mohan Tallapragada¹, Alice Branton¹, Dahryn Trivedi¹, Gopal Nayak¹, Omprakash Latiyal², Snehasis Jana^{2,*}

¹Trivedi Global Inc., Henderson, USA

²Trivedi Science Research Laboratory Pvt. Ltd., Bhopal, Madhya Pradesh, India

Email address:

publication@trivedisrl.com (S. Jana)

To cite this article:

Mahendra Kumar Trivedi, Rama Mohan Tallapragada, Alice Branton, Dahryn Trivedi, Gopal Nayak, Omprakash Latiyal, Snehasis Jana. Evaluation of Atomic, Physical, and Thermal Properties of Bismuth Oxide Powder: An Impact of Biofield Energy Treatment. *American Journal of Nano Research and Applications*. Vol. 3, No. 6, 2015, pp. 94-98. doi: 10.11648/j.nano.20150306.11

Abstract: Bismuth oxide (Bi_2O_3) is known for its application in several industries such as solid oxide fuel cells, optoelectronics, gas sensors and optical coatings. The present study was designed to evaluate the effect of biofield energy treatment on the atomic, physical, and thermal properties of Bi_2O_3 . The Bi_2O_3 powder was equally divided into two parts: control and treated. The treated part was subjected to biofield energy treatment. After that, both control and treated samples were investigated using X-ray diffraction (XRD), thermogravimetric analysis (TGA), Fourier transform infrared (FT-IR) spectroscopy, and electron spin resonance (ESR) spectroscopy. The XRD data exhibited that the biofield treatment has altered the lattice parameter (-0.19%), unit cell volume (-0.58%), density (0.59%), and molecular weight (-0.57%) of the treated sample as compared to the control. The crystallite size was significantly increased by 25% in treated sample as compared to the control. Furthermore, TGA analysis showed that control and treated samples were thermally stable upto tested temperature of 831°C. Besides, the FT-IR analysis did not show any significant change in absorption wavenumber in the treated sample as compared to the control. The ESR study revealed that g-factor was increased by 13.86% in the treated sample as compared to the control. Thus, above data suggested that biofield energy treatment has altered the atomic and physical properties of Bi_2O_3 . Therefore, the biofield treated Bi_2O_3 could be more useful in solid oxide fuel cell industries.

Keywords: Bismuth Oxide, Biofield Energy Treatment, X-ray Diffraction, Differential Scanning Calorimetry, Thermogravimetric Analysis, Fourier Transform Infrared Spectroscopy

1. Introduction

Bismuth oxide (Bi_2O_3) is known for its optical and electrical properties such as dielectric permittivity, refractive index, large energy band gap, photoconductivity and photoluminescence [1]. Due to these properties, Bi_2O_3 play a vital role in the various fields such as optoelectronics, gas sensors and optical coatings. Bi_2O_3 has five polymorphs *i.e.* α - Bi_2O_3 (monoclinic), β - Bi_2O_3 (tetragonal), γ - Bi_2O_3 (BCC), δ - Bi_2O_3 (Cubic), and ϵ - Bi_2O_3 (triclinic) [2]. Among these phase, α - Bi_2O_3 and δ - Bi_2O_3 are the stable phases, while rest other phases are metastable. Furthermore, δ - Bi_2O_3 exists in the form of face centered cubic crystal structure [3]. The δ - Bi_2O_3 is known for its high conductivity among all other phases, which make it best material in solid oxide fuel cell. Although its application as

oxide ion conductor is limited, because it is only stable in the narrow temperature range. Recently, the stability of δ - Bi_2O_3 is reported to be increased by various kind of dopants such as Er_2O_3 [4] and Y_2O_3 [5] etc. Verkerk *et al.* reported that erbia-stabilized bismuth oxides are among the best solid oxide oxygen ion conductors [6]. In numerous research, the stabilization of the δ - Bi_2O_3 was enhanced by doping with 20 to 50% lanthanide ions [7-9]. However, all these process are either required costly equipment setup or high temperature devices. Thus, it is important to study an alternative approach *i.e.* biofield energy treatment, which could modify the Bi_2O_3 with respect to its atomic, physical, thermal properties. Recently, the biofield energy treatment has gained significant attention, due to its ability to alter the physical, atomic, and structure properties of metals [10, 11] and ceramics [12, 13].

Furthermore, a human has the capability to harness the energy from the environment/Universe and transmit it to any object around the Globe. The object(s) receive the energy and respond into a useful way that is called biofield energy, and this process is known as biofield energy treatment. Besides, the National Center for Complementary and alternative medicine (NCCAM) has recommended uses of CAM therapies (*e.g.* healing therapy) in the healthcare sector [14]. Nevertheless, Mr. Trivedi's unique biofield energy treatment (The Trivedi Effect[®]) had altered the atomic, physical and thermal characteristics in several ceramics oxides [15,16]. Thus, after considering the excellent outcomes with biofield energy treatment on ceramics and the industrial applications of Bi₂O₃, this work was undertaken to evaluate the effect of this treatment on the atomic, physical and thermal properties of the Bi₂O₃ using X-ray diffraction (XRD), thermogravimetric analysis (TGA), Fourier transform infrared (FT-IR) spectroscopy and electron spin resonance (ESR) spectroscopy.

2. Materials and Methods

The Bi₂O₃ powder was procured from Sigma Aldrich, USA. The procured powder was equally divided into two parts and coded as control and treated. The control part was remained the same and the treated part was in sealed pack, handed over to Mr. Trivedi for biofield energy treatment under standard laboratory conditions. Mr. Trivedi provided the treatment through his energy transmission process to the treated sample without touching the sample. After that, the control and treated samples were characterized using XRD, TGA, FT-IR and ESR techniques.

2.1. XRD Study

The XRD analysis of control and treated Bi₂O₃ was accomplished on Phillips, Holland PW 1710 X-ray diffractometer system. The X-ray of wavelength 1.54056×10^{-10} m was used. From the XRD diffractogram, the peak intensity counts, *d* value (Å), full width half maximum (FWHM) (θ°), relative intensity (%) values were obtained. The PowderX software was used to compute the lattice parameter and unit cell volume of the control and treated Bi₂O₃ samples. The crystallite size (*D*) was calculated by using Scherrer equation as following:

$$D = k\lambda / (b \cos \theta)$$

Here, *b* is full width half maximum (FWHM) of XRD peaks, *k*=0.94, and $\lambda = 1.54056$ Å.

The percentage change in crystallite size was calculated using following formula:

$$\% \text{ change in crystallite size} = [(D_t - D_c) / D_c] \times 100$$

Where, *D_c* and *D_t* are crystallite size of control and treated powder samples respectively.

2.2. Thermal Analysis

The thermal analysis of Bi₂O₃ powder was done using

TGA-DTG. For that, Mettler Toledo simultaneous TGA-DTG instrument was used. The samples were heated from room temperature to 900°C with a heating rate of 10°C/min under nitrogen atmosphere.

2.3. FT-IR Spectroscopy

The FT-IR analysis of control and treated Bi₂O₃ samples were carried out on Shimadzu's FT-IR (Japan) with frequency range of 4000-500 cm⁻¹. The analysis was accomplished to evaluate the effect of biofield treatment on dipole moment, force constant and bond strength in chemical structure.

2.4. ESR Spectroscopy

The ESR analysis of control and treated Bi₂O₃ samples were performed on Electron Spin Resonance (ESR), E-112 ESR Spectrometer of Varian USA. In this experiment, X-band microwave frequency (9.5 GHz), having sensitivity of 5×10^{10} , Δ*H* spins was used.

3. Results and Discussion

3.1. XRD Study

The XRD is a quantitative and non-destructive technique, which have been widely used to study the crystal structure parameters of a compound. Figure 1 shows the XRD diffractogram of control and treated Bi₂O₃ samples. It can be observed that the control sample showed the crystalline peaks at Bragg angle (2θ) 27.08°, 27.68°, 32.70°, 32.93°, 34.70°, 37.24°, 46.03°, and 52.08°. However, the treated sample showed the peaks at Bragg's angle 27.17°, 27.79°, 32.82°, 33.03°, 34.84°, 37.39°, 46.09°, and 52.17°. It indicated that the XRD peaks were shifted toward higher angles in the treated sample as compared to control, after biofield energy treatment. It is reported that the reduction in lattice parameter and unit cell volume lead to shifting of the XRD peaks toward higher angles [17]. The XRD data of the control and treated samples were analyzed using PowderX software. The crystal structure parameters such as lattice parameter, unit cell volume, density, and molecular weight were computed and presented in Table 1. The data showed that the lattice parameter of treated sample was decreased from 5.6596 Å to 5.6487 Å. Kumar *et al.* reported that the XRD peaks can shift to the higher side if larger radii atoms are replaced by smaller radii atoms [18].

Nevertheless the unit cell volume of treated Bi₂O₃ powder was decreased by 0.58% as compared to control. Thus, the decrease in lattice parameter and unit cell volume were supported by shifting of XRD peaks toward higher angles. Hence, based on shifting of XRD peaks and reduction in the lattice parameter, it is assumed that the biofield treatment might induce compressive stress in treated Bi₂O₃ powder and this might be responsible for the internal strain in treated Bi₂O₃. Ekhekar *et al.* reported that the lattice parameter of Bi₂O₃ unit cell was reduced from 5.560 Å to 5.540 Å when the doping composition of Y₂O₃ was increased from 10 to 20% in Bi₂O₃ and increased the stability of δ- Bi₂O₃ [19]. Thus, it is

assumed that the decrease in lattice parameter of Bi_2O_3 after biofield treatment might increase the stability of δ - Bi_2O_3 . Moreover, the reduction in unit cell volume led to the increase in density of treated Bi_2O_3 powder by 0.59% as compared to the control. The molecular weight of the treated Bi_2O_3 powder was reduced by 0.57% as compared to the control. Besides, the crystallite size of treated Bi_2O_3 was increased from 85.10 nm (control) to 106.39 nm after biofield treatment. It indicated that the crystallite size was significantly increased by 25% as compared to the control. It is possible that the neighboring crystalline plane reoriented themselves in the same plane and increased the crystallite size. Li *et al.* reported that the

crystallite size of Bi_2O_3 containing compound was increased with increased in sintering time [20]. It is also mentioned that the increase in crystallite size caused an increase in ionic conductivity in Bi_2O_3 . Thus, based on this, it is assumed that the increase in crystallite size in treated Bi_2O_3 may lead to increase the ionic conductivity. It could be due to the reduction of crystallite boundaries in treated Bi_2O_3 as compared to control since an increase in crystallite size decrease the crystallite boundaries. Therefore, the increase in ionic conductivity and stability of Bi_2O_3 could play a major role in the enhancement of efficiency of the solid oxide fuel cell.

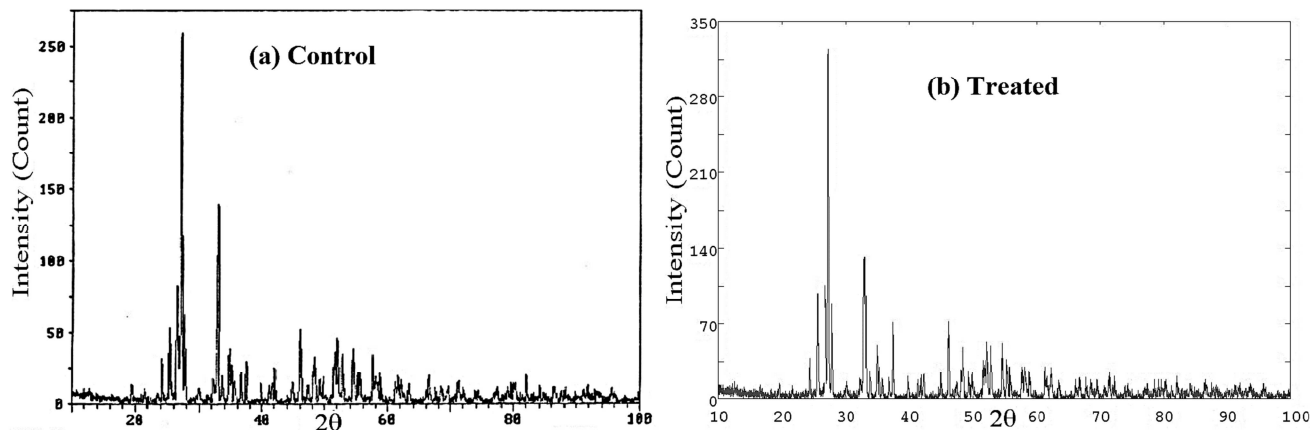


Fig. 1. X-ray diffractogram of bismuth oxide powder.

Table 1. Effect of biofield energy treatment on lattice parameter, unit cell volume density, molecular weight, and crystallite size of bismuth oxide powder.

| Group | Lattice parameter (Å) | Unit cell volume ($\times 10^{-23} \text{ cm}^3$) | Density (g/cc) | Molecular weight (g/mol) | Crystallite size (nm) |
|----------|-----------------------|---|----------------|--------------------------|-----------------------|
| Control | 5.6596 | 18.13 | 8.6097 | 470.04 | 85.10 |
| Treated | 5.6487 | 18.02 | 8.6599 | 467.32 | 106.39 |
| % Change | -0.19 | -0.58 | 0.59 | -0.57 | 25 |

3.2. Thermal Analysis

The analysis result of TGA are presented in Table 2. The data exhibited that both the control and treated sample were started weight loss at temperature around 50°C. The control sample lost around 0.22% upto temperature 335°C. After that, the control sample started to gain the weight and which led to increase the weight by 0.2% upto temperature 821°C and so on. It indicated that control sample was thermally stable. However, the treated sample started to lose its weight at 50°C that continued till 660°C. In this process, the sample lost around 1.7% of its initial weight. The weight loss in temperature upto 335°C in control and treated sample could be due to the elimination of water from the samples. Klinkova *et al.* had studied the thermal behavior of Bi_2O_3 , where it was reported that the sample continue to show weak weight loss upto 600°C due to the removal of oxygen. It was also mentioned that the formula unit was changed to $\text{Bi}_2\text{O}_{2.902}$ after heating of the sample upto 600°C [21]. Furthermore, the weight loss observed in control and treated samples were less than 1.7% which may be due to the loss of oxygen or water, thus, it indicated that both samples were thermally stable.

Table 2. TGA analysis of bismuth oxide powder.

| Parameter | Control | Treated |
|-------------------------|---------|---------|
| Onset temperature (°C) | 50 | 50 |
| Endset temperature (°C) | 335 | 660 |
| Percent weight loss (%) | 0.22 | 1.7 |

3.3. FT-IR Spectroscopy

The FT-IR spectra of control and treated Bi_2O_3 samples are presented in Figure 2. The band observed at around 3439 cm^{-1} in both control and treated samples could be due to O-H stretching vibrations indicating the presence of the water molecule. In addition, the band was observed in the range $400\text{-}700 \text{ cm}^{-1}$ i.e. 440 and 506 cm^{-1} in control and treated sample could be the characteristics vibrations of Bi-O bond [22]. In addition, Wang *et al.* also reported the Bi-O stretching vibrations at 515 cm^{-1} [23]. Thus, the FT-IR data did not show any significant alteration in absorption wavenumbers of treated sample as compared to the control.

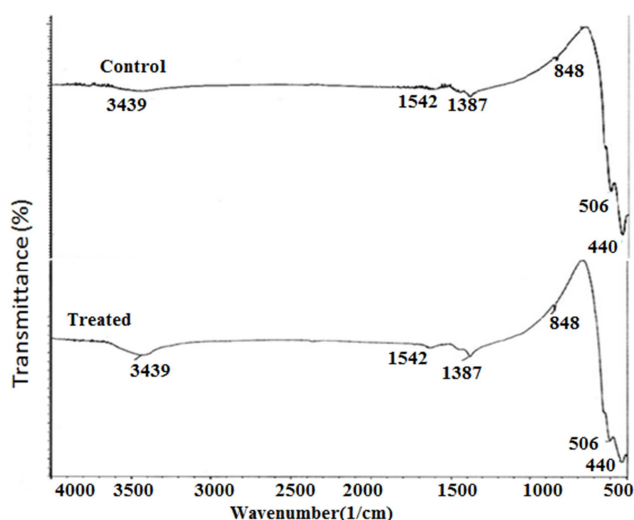


Fig. 2. FT-IR spectra of bismuth oxide powder.

3.4. ESR Spectroscopy

The analysis result of control and treated Bi_2O_3 samples using ESR are illustrated in Table 3. The data showed that the g-factor was increased from 2.0054 (control) to 2.2833 in treated Bi_2O_3 sample. It suggested that the g-factor was increased by 13.86% in treated sample as compared to the control. Also, the width and height of the ESR signal were significantly increased by 311.1 and 1188.9% respectively, as compared to the control. Thus, the increase in ESR signal width and height indicated that the interaction of electron with neighboring elements in treated sample probably altered after biofield treatment. It is assumed that the biofield energy, which probably transferred through treatment, possibly acted at atomic level to cause these modifications.

Table 3. Effect of biofield energy treatment on the ESR properties of bismuth oxide.

| Group | g-factor | ESR signal width | ESR signal height |
|----------------|----------|------------------|-----------------------|
| Control | 2.0054 | 90 | 1.41×10^{-4} |
| Treated | 2.2833 | 370 | 1.81×10^{-3} |
| Percent Change | 13.86 | 311.1 | 1188.9 |

4. Conclusions

The XRD data revealed that the lattice parameter was reduced in treated sample as compared to the control. The decrease in lattice parameter may lead to enhance the stability of δ - phase of Bi_2O_3 in treated sample as compared to the control. Also, the increase in crystallite size upto 25% suggest that the ionic conductivity of treated Bi_2O_3 might increase after biofield treatment. The TGA study showed the stability of control and treated Bi_2O_3 samples upto the tested temperature of 900°C . Besides, the ESR spectra study revealed that the signal width and height were significantly increased by 311.1 and 1188.9% respectively, as compared to the control. Thus, overall study concludes that biofield

treatment has altered the atomic and physical properties of Bi_2O_3 . Therefore, the treated Bi_2O_3 could be more beneficial in solid oxide fuel cell as compared to the control.

Acknowledgments

Authors would like to acknowledge Dr. Cheng Dong of NLSC, Institute of Physics, and Chinese academy of sciences for permitting us to use Powder-X software for analyzing XRD results. The authors would also like to thank Trivedi Science, Trivedi Master Wellness and Trivedi Testimonials for their support during the work.

References

- [1] Oudghiri-Hassani H, Rakass S, Al Wadaani FT, Al-ghamdi KJ, Omer A, et al. (2015) Synthesis, characterization and photocatalytic activity of α - Bi_2O_3 nanoparticles. J Taibah Univ Sci 9: 508-512.
- [2] Fan HT, Pan SS, Teng XM, Ye C, Li HG, et al. (2006) δ - Bi_2O_3 thin films prepared by reactive sputtering: Fabrication and characterization. Thin Solid Films 513:142-147.
- [3] Kayali R, Kasikci M, Durmus S, Ari M (2011) Investigation of electrical, structural and thermal stability properties of cubic $(\text{Bi}_2\text{O}_3)_{1-x-y}(\text{Dy}_2\text{O}_3)_x(\text{Ho}_2\text{O}_3)_y$ ternary system. Fuel Cells 1219-1234.
- [4] Vinke IC, Seshan K, Boukamp BA, Vries KJ de, Burggraaf AJ (1989) Electrochemical properties of stabilized δ - Bi_2O_3 . Oxygen pump properties of Bi_2O_3 - Er_2O_3 solid solutions. Solid State Ionics 34: 235-242.
- [5] Battle PD, Catlow CRA, Heap JW, Moroney LM (1986) Structural and dynamical studies of δ - Bi_2O_3 oxide ion conductors: I. The structure of $(\text{Bi}_2\text{O}_3)_{1-x}(\text{Y}_2\text{O}_3)_x$ as a function of x and temperature. J Solid State Chem 63: 8-15.
- [6] Verkerk MJ, Keizer K, Burggraaf AJ (1980) High oxygen ion conduction in sintered oxides of the Bi_2O_3 - Er_2O_3 system. J Appl Electrochem 10: 81-90.
- [7] Tanabe H, Fukushima S (1986) Cathodic polarization characteristics of the oxygen electrodes/stabilized Bi_2O_3 solid electrolyte interface. Electrochem Acta 31: 801-809.
- [8] Esaka T, Iwahara H, Kunieda H (1982) Oxide ion and electron mixed conduction in sintered oxides of the system Bi_2O_3 - Pr_6O_{11} . J Appl Electrochem 12: 235-240.
- [9] Battle PD, Catlow CRA, Chadwick AV, Cox P, Greaves GN, et al. (1987) Structural and dynamical studies of δ - Bi_2O_3 oxide ion conductors: IV. An EXAFS investigation of $(\text{Bi}_2\text{O}_3)_{1-x}(\text{M}_2\text{O}_3)_x$ for M = Y, Er, and Yb. J Solid State Chem 69: 230-239.
- [10] Trivedi MK, Tallapragada RM, Branton A, Trivedi D, Nayak G, et al. (2015) Potential impact of biofield treatment on atomic and physical characteristics of magnesium. Vitam Miner 3: 129.
- [11] Trivedi MK, Nayak G, Patil S, Tallapragada RM, Latiyal O, et al. (2015) An evaluation of biofield treatment on thermal, physical and structural properties of cadmium powder. J Thermodyn Catal 6: 147.

- [12] Trivedi MK, Nayak G, Patil S, Tallapragada RM, Latiyal O, et al. (2015) Impact of biofield treatment on atomic and structural characteristics of barium titanate powder. *Ind Eng Manage* 4: 166.
- [13] Trivedi MK, Patil S, Nayak G, Jana S, Latiyal O (2015) Influence of biofield treatment on physical, structural and spectral properties of boron nitride. *J Material Sci Eng* 4: 181.
- [14] Barnes PM, Powell-Griner E, McFann K, Nahin RL (2004) Complementary and alternative medicine use among adults: United States, 2002. *Adv Data* 343: 1-19.
- [15] Trivedi MK, Nayak G, Patil S, Tallapragada RM, Latiyal O (2015) Studies of the atomic and crystalline characteristics of ceramic oxide nano powders after bio field treatment. *Ind Eng Manage* 4: 161.
- [16] Trivedi MK, Nayak G, Patil S, Tallapragada RM, Latiyal O (2015) Impact of biofield treatment on physical, structural and spectral properties of antimony sulfide. *Ind Eng Manage* 4:165.
- [17] Schwertmann U, Cornell RM (2007) Iron oxides in the laboratory: preparation and characterization. John Wiley & Sons.
- [18] Kumar P, Kar M (2014) Effect of structural transition on magnetic and dielectric properties of La and Mn co-substituted BiFeO₃ ceramics. *Mater Chem Phys*. 148: 968-977.
- [19] Ekhekar S, Bichile GK (2004) Synthesis and structural characterization of (Bi₂O₃)_{1-x}(Y₂O₃)_x and (Bi₂O₃)_{1-x}(Gd₂O₃)_x solid solutions. *Bull Mater Sci* 27: 19-22.
- [20] Li R, Zhen Q, Drache M, Rubbens A, Estournès C, et al (2011) Synthesis and ion conductivity of (Bi₂O₃)_{0.75}(Dy₂O₃)_{0.25} ceramics with grain sizes from the nano to the micro scale. *Solid State Ionics* 198: 6-15.
- [21] Klinkova LA, Nikolaichik VI, Barkovskii NV, Fedotov VK (2007) Thermal stability of Bi₂O₃. *Russ J Inorg Chem* 52: 1822-1829.
- [22] Mallahi M, Shokuhfar A, Vaezi MR, Esmaeilirad A, Mazinani V (2014) Synthesis and characterization of bismuth oxide nanoparticles via sol-gel method. *AJER* 3: 162-165.
- [23] Wang SX, Jin CC, Qian WJ (2014) Bi₂O₃ with activated carbon composite as a supercapacitor electrode. *J Alloy Compd* 615: 12-17.